Pis'ma v ZhETF, vol. 97, iss. 7, pp. 458 – 464 © 2013 April 10

Ab initio study of surface electronic structure of phosphorus donor imputiry on Ge(111)-(2×1) surface

S. V. Savinov[1)], *A. I. Oreshkin*, *S. I. Oreshkin*[+]

Department of Physics, Lomonosov Moscow State University, 119991 Moscow, Russia

[+]*Sternberg Astronomical Institute, Moscow State University, 119991 Moscow, Russia*

Submitted 28 January 2013

We present the results of numerical modeling of Ge(111)-(2×1) surface electronic properties in vicinity of P donor impurity atom near the surface. We show, that despite of well established bulk donor impurity energy level position at the very bottom of conduction band, surface donor impurity might produce energy level below Fermi energy, depending on impurity atom local environment. It was demonstrated, that impurity, located in subsurface atomic layers, is visible in STM experiment. The quasi-1D character of impurity image, observed in STM experiments, is confirmed by our computer simulations.

DOI: 10.7868/S0370274X13070047

Introduction. The reliable STM image interpretation still remains the challenging task. There is no general approach which takes into account all kind of physical processes responsible for STM image formation. Below we report on surface electronic structure investigation performed by *ab initio* computer simulations in the density functional framework, which is the first order estimation for STM images, and could serve as a basis for further model improvements.

We have done our DFT calculations in LDA approximation as implemented in SIESTA [1] package. Details can be found elsewhere [2]. The use of strictly localized numerical atomic orbitals is necessary to be able to finish the modeling of large surface cell in finite time. The surface Ge(111)-(2×1) super-cell consists of 7×21 cells of elementary 2×1 reconstruction, each 8 Ge atomic layers thick (total 2646 atoms). Vacuum gap is chosen rather big – about 20 Å. Ge dangling bonds at the slab bottom surface are terminated with H atoms to prevent surface states formation. The geometry of the structure was fully relaxed, until atomic forces have became less then 0.003 eV/Å.

We restrict the present investigation to the case of left (negative) only surface buckling as at present this matter is still controversial and is the subject of intensive investigations [3–5]. Our research is in some sense similar to reported in [6, 7] for Si(111)-(2×1) surface. But we take into account all possible impurity positions in two surface bi-layers of Ge(111)-(2×1) reconstruction, and besides, our analysis is not aimed on pure STM image simulation, rather on comprehensive analyses of local density of states.

As we have reported earlier, the atomic structure of Ge(111)-(2×1) surface is strongly disturbed around surface defects [2]. That is why the geometry relaxation has been performed with the big super-cell to keep the internally periodic images of impurity well separated. Although it is still the open question, if the defect's images separation is sufficiently large. At the last step

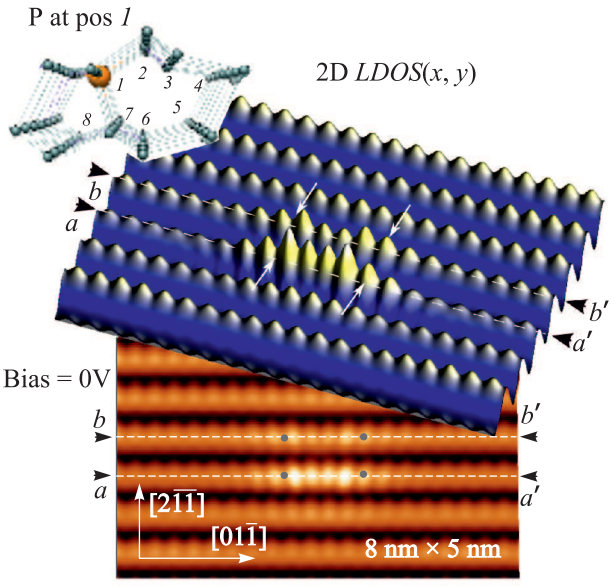

Fig. 1. Labels to mark donor atom position in two surface bi-layers of Ge(111)-(2×1) reconstruction. P atom is shown in position *1*. Quasi-3D and 2D representations of $LDOS(x, y)|_{eV=0}$ field at zero bias

[1)]e-mail: SavinovSV@mail.ru

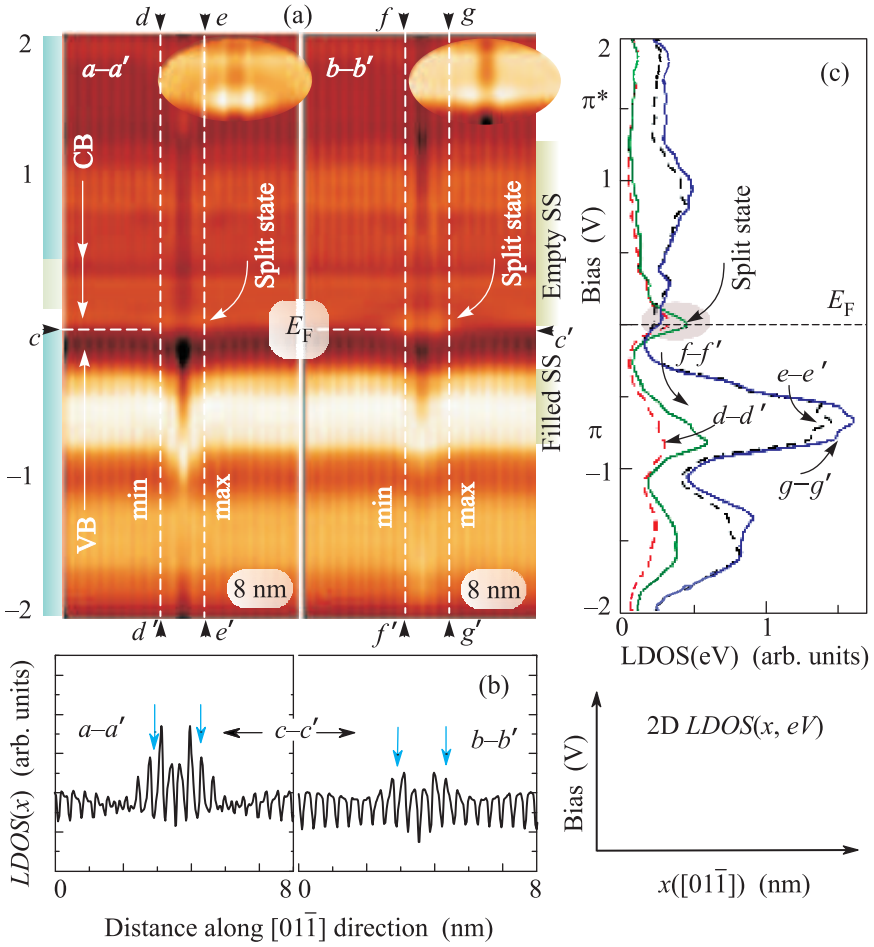

Fig. 2. (a) – 2D $LDOS(x, eV)$ distributions taken along a–a' and b–b' *planes* in Fig. 1. (b) – Profiles of a–a' and b–b' panes along c–c' line, which are *essentially the same* as profiles of images in Fig. 1 along a–a' and b–b' *lines*. (c) – Profiles of a–a' and b–b' images along d–d', e–e', f–f' and g–g' lines, which are $LDOS(eV)$ dependencies at points, shown in Fig. 1 by black dots and white arrows

of simulation the spatial distribution of Khon–Sham wave-functions and corresponding scalar field of surface electronic density of states $LDOS(x, y, eV)$ were calculated. Because of strictly localized atomic orbitals, used in SIESTA, the special procedure of wave-functions extrapolation into the vacuum has to be used (it is also implemented in SIESTA package).

1. Surface local density of states. Importantly, the STM is measuring $LDOS$ *above* the surface, and thus in our DFT calculations we are interested in the following quantity:

$$LDOS(x, y, eV) = \sum |\Psi(x, y)|^2 \, \tilde{\delta}(E - E_i)|_{z=\text{const}},$$

where eV is tunneling bias voltage, Ψ are Khon–Sham eigenfunctions, $\tilde{\delta}$ is finite width smearing function, E_i are Khon–Sham eigenvalues, and summing is evaluated at certain plane (z = const), located a few angstroms above the surface. In further exposition we will focus mostly on $LDOS$ properties.

Before we go to the main results we have to clarify the physical meaning of our data representation.

Everywhere below we are speaking about cross-sectioning of $LDOS(x, y, eV)$ scalar field. The x and y directions correspond to [01$\bar{1}$] and [2$\bar{1}\bar{1}$] crystallographic directions. The two most relevant quantities are cross-section of scalar field $LDOS(x, y, eV)$ along (x, y) and (x, eV) planes – $LDOS(x, y)$ and $LDOS(x, eV)$ respectively.

In Fig. 1 we show the cross-sections at fixed bias voltage $LDOS(x, y)|_{eV=0}$ for the case of P atom located at position *1* in surface bi-layer. These images roughly correspond to experimental STM images, as at small bias voltage there are not too many sharp $LDOS$ features, contributing to the image. It can be seen from Fig. 1, *two* π-bonded rows of surface reconstruction are influenced

by impurity. In each row a protrusion can be observed. The spatial extent of impurity induced feature along the direction of π-bonded dimer row ($[01\bar{1}]$ direction) is at least 40 Å. Note two distinguishable maxima on the protrusion. We will come back to this fact later. Arrows and dots on the image, as well as (a–a') and (b–b') lines, mark spatial points and directions, referred in Fig. 2.

In Fig. 2a the cross-sections at fixed y coordinate $LDOS(x, eV)|_{a-a'(b-b')}$ are shown. They are taken along (a–a') and (b–b') *planes* in Fig. 1, i.e. along π-bonded rows of Ge(111)-(2×1) reconstruction. The additional, comparing to the case of clean Ge(111)-(2×1) surface, energy level appears at Fermi energy. We will refer to it as to split state. Areas, where split state resides, are zoomed in on the insets. The positions of Fermi level E_F, conduction band (CB) bottom, valence band (VB) top and empty π^* and filled π surface states bands are indicated in Fig. 2. According to DFT calculations the top of VB coincide with the bottom of empty surface states band π^* and Fermi level [2]. Even more, the π^* band can be partially filled at very high doping ratio [8].

The proportions of $LDOS(x, eV)$ images are chosen on purpose in a way that is convenient for experimenters. Typically the number of points along spatial direction is less than the number of bias voltage points and tunneling spectra image is elongated in vertical (eV) direction.

It is necessary to state, that everywhere below the bottom of CB is schematically shown on the figures for the case of Ge(111)-(2×1) surface at room temperature. In this case the optical band gap is about 0.5 eV [9]. The DFT band gap in LDA approximation is non-physically small, less then 100 meV. It is shown in Fig. 2a by additional rectangle. It is really difficult to define the energetic position reference level, is it Fermi energy, or the CB bottom? Energetically the split state is aligned with empty surface states π^* band bottom. To be accurate we will refer to the Fermi level, i.e. split state is located at the Fermi level, and not near CB bottom.

The distribution $LDOS(x, eV)$ is reach of features. Its cross-section along x coordinate gives the $LDOS(x)$ profile *exactly* in the same way as the cross-sectioning of $LDOS(x, y)$ (Fig. 1) along x coordinate. The cross-sections of a–a' and b–b' panes along c–c' line are shown on the panel (b). One can see two maxima on the profiles. And what is really important is that the spatial extent of perturbation is obviously about 80 Å. The previous common sense 40 Å estimation was wrong simply due to the insufficient visual contrast of $LDOS(x, y)|_{eV=0}$ image, which was set with typical "full height = full color" coloring scheme.

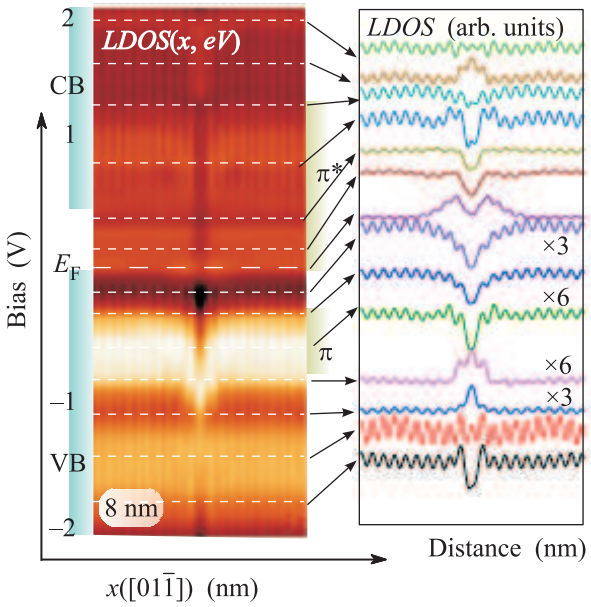

Fig. 3. $LDOS(x, eV)$ map along b–b' line in vicinity of P atom, located at positions *1* on Ge(111)-(2×1) surface and its cross-sections along denoted lines

Cross-section of $LDOS(x, eV)$ along eV coordinate (d–d', e–e', f–f' and g–g' lines Fig. 2a) corresponds to point spectroscopy $LDOS(eV)$ dependencies (Fig. 2c) at points of $LDOS(x)$ profile, marked by vertical arrows in Fig. 2b. These are points shown in Fig. 1 by dots and arrows.

Curves d–d' and f–f' are taken in between dimers in π-bonded row, while curves e–e' and g–g' are taken on top of dimers (Fig. 2b and 1). For the whole range of bias voltage the values of $LDOS$ collected in between dimer are higher than that on top of dimers, except for narrow interval in vicinity of Fermi energy, where resides the split state. This split state contribute to the increase of $LDOS$ on top of dimers in π-bonded row. Thus the protrusion, consisting of few dimers appear on $LDOS(x, y)$ (as well as on STM) image. It follows from Fig. 2c that the contrast of protrusion is higher on (a–a') plane than on (b–b') plane, and this indeed can be observed in Fig. 1.

To clarify the meaning of $LDOS(x, eV)$ map the set of cross-sections along x spatial coordinate is depicted in Fig. 3 for P donor atom located at position *1*. Profiles are slightly low pass filtered to stress the long range features, so they look a bit different comparing to Fig. 2b. When tunneling bias changes, the $LDOS(x)$ profile also changes revealing deeps and protrusions of different shape. The profile, corresponding to split state energy (and to the presence of protrusion on STM image) is marked by ellipse. One can easily see that the am-

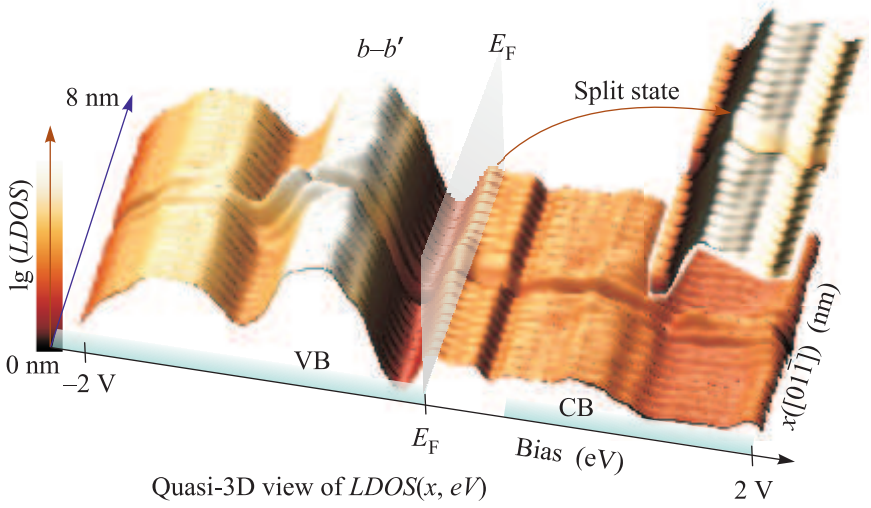

Fig. 4. Quasi-3D representation of $LDOS(x, eV)$ along central π-bonded row of Fig. 1. Area, containing split state is zoomed in to give clear impression about its spatial structure. Fermi level is shown as semitransparent plane

plitude of protrusion at Fermi level is much smaller than the amplitude of features at other bias voltage (see also Fig. 2c). Also note, that impurity's $LDOS$ image might has hillock like shape at positive bias (empty states). It means the protrusion on the $LDOS$ image is not caused by charge density effects (like charge screening).

To the best of our knowledge this fact was never clearly stated. In other words, STM image of Ge(111)-(2×1) surface (as well as Si(111)-(2×1) surface [6, 7]) in vicinity of Fermi level is dominated by the split state, although the amplitude of the effect is relatively small.

To give even more insight into the power of $LDOS(x, eV)$ data representation it is drawn in Fig. 4 as quasi-3D surface. Height is given on logarithmic scale to increase the image height contrast. The value of LDOS is coded both by height and by color with lightning. The spatial and energetic positions of specific features of tunneling spectrum can be easily deduced from the figure. The split state (zoomed in on the inset) is located at Fermi level. It has cigar like spatial shape which directly reflects in the shape of protrusion on $LDOS(x, y)$ image.

It is also obvious from Fig. 4, that split state really fills in the whole width of $LDOS(x, eV)$ spectra. Thus we can not completely exclude the possibility of impurity induced electronic features overlap between neighboring super-cells of calculation. As the quantum mechanical forces are calculated as gradients of electronic density, the overlap can introduce some difficult to estimate errors. This is the main reason, why we have increased the size of geometry relaxation surface cell to the upper available to us limit.

Taking stated above into account one can conclude that, given $LDOS(x, eV)$ it is readily possible to estimate the outlook of point spectroscopy curves as well as the shape of spatial profiles. That is why the results of electronic properties calculations for all 8 possible positions of P impurity atom in two surface bi-layers (see Fig. 1) are presented in Fig. 5 as $LDOS(x, eV)$ maps.

Let us point out the most important features of calculated images. As we have already discussed the empty surface states band π^* is governing STM image formation in vicinity of Fermi level for Ge(111)-(2×1) surface [2, 8]. The split state is formed due to strong atomic orbitals hybridization [2] in vicinity of atomic defect. For all P doping atom positions except position 3, the split state is located at the Fermi level, which almost coincide with π^* empty surface band bottom. When P impurity is placed at position *3*, the split state can be observed below Fermi energy Fig. 5(*3*). Position *2* is somewhat specific. In this case the impurity atom is directly breaking π-bonded chain, and this strongly influences $LDOS(x, eV)$ (Fig. 5(*2*)) – at almost all possible bias voltage values the impurity LDOS image has two well pronounced peaks.

The noticeable influence of surface states can be inferred from Fig. 5. There are $LDOS$ peaks near the top of empty surface states band π^* and at the top of filled surface states band π. They are imaged as horizontal bright stripes (Fig. 5).

The atomic orbitals in vicinity of surface defects are strongly hybridized. This results in up/downward band edges "bending". The insets of Fig. 5 with split state areas zoomed in with high contrast, illustrates this. Basi-

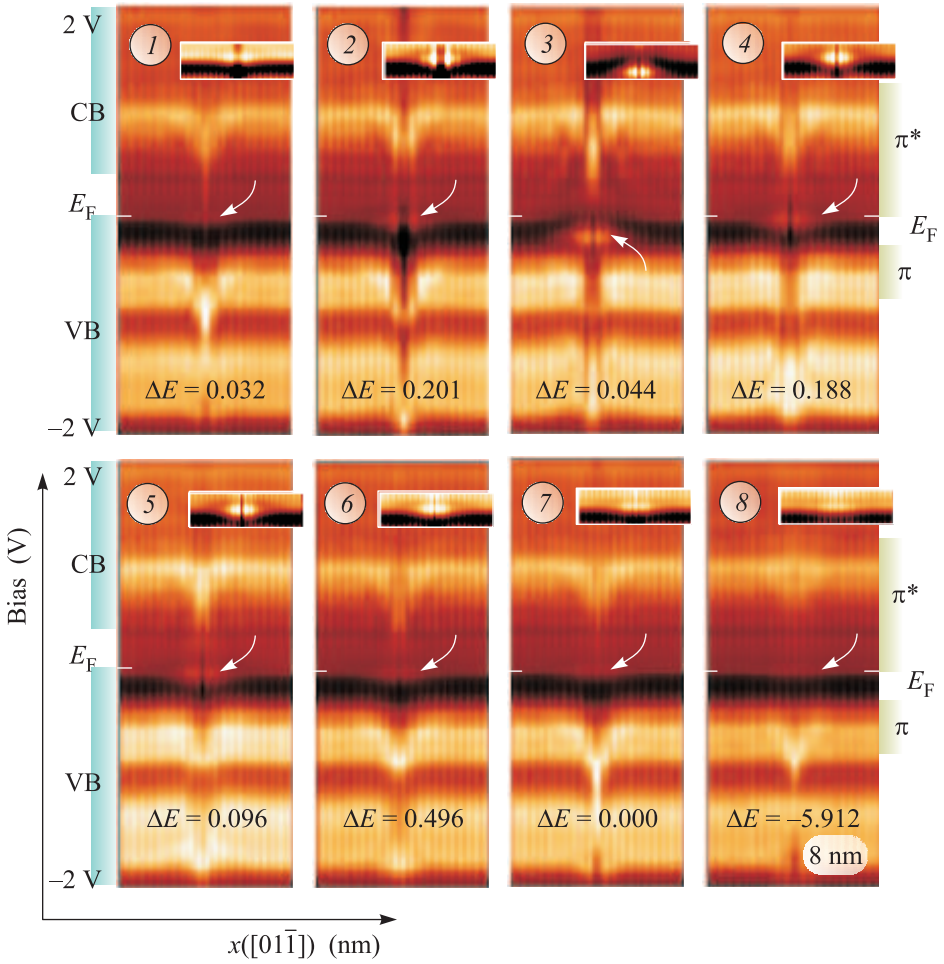

Fig. 5. $LDOS(x, eV)$ maps in vicinity of P atom, located at different positions in subsurface layers of Ge(111)-(2×1) surface. Numbers denote atom position. Energy difference in eV relative to position *7* as well as Fermi level position and split state position are indicated in the figure. Area of split state is zoomed in on every pane

cally, the orbital's hybridization leads to specific spatial shape of tunneling spectra $LDOS(x, eV)$ and, in other words, to the appearance of local electronic density spatial oscillations [2]. Let us note, these are not charge density oscillations, because they are observed in empty states energy range (above Fermi level). Spatial *LDOS* oscillation on Ge(111)-(2×1) surface were the subject of [10] work.

The energy difference, measured with respect to the total energy of a system with P donor atom at position *7*, is large for donor positions *8*. We do not have any explanation for huge energy gain for impurity position *8*. At the same time this energy difference apply to surface slab consisting of 2646 atoms. Due to slightly different atoms relaxation a few electronvolts can easily be acquired by the whole super-cell.

The *LDOS* (and STM) image of individual impurity is dominated by the split state at zero (Fig. 1) and low negative bias (see above) voltage as illustrated by Fig. 6, where zero bias maps of $LDOS(x, y)|_{eV=0}$ for different donor atom positions are presented together with corresponding quasi-3D images. The profiles along b–b' direction are shown on the maps on the same scale. Three things can be noticed from Fig. 6. Firstly, one or two π-bonded rows are affected by donor impurity. Secondly, one or two local maxima are present on the profile. Thirdly, the distance between maxima can be one or two dimers along π-bonded row ($[01\bar{1}]$ direction). This is shown in Fig. 6 by thin lines and arrows and is summarized in Table.

P donor impurity *LDOS* image properties

Atom position	*1*	*2*	*3*	*4*	*5*	*6*	*7*	*8*
2 rows	*x*	–	–	–	–	*x*	*x*	*x*
2 max	*x*	*x*	*x*	*x*	*x*	–	*x*	*x*
Num. dimers	2	2	1	1	1	–	2	1

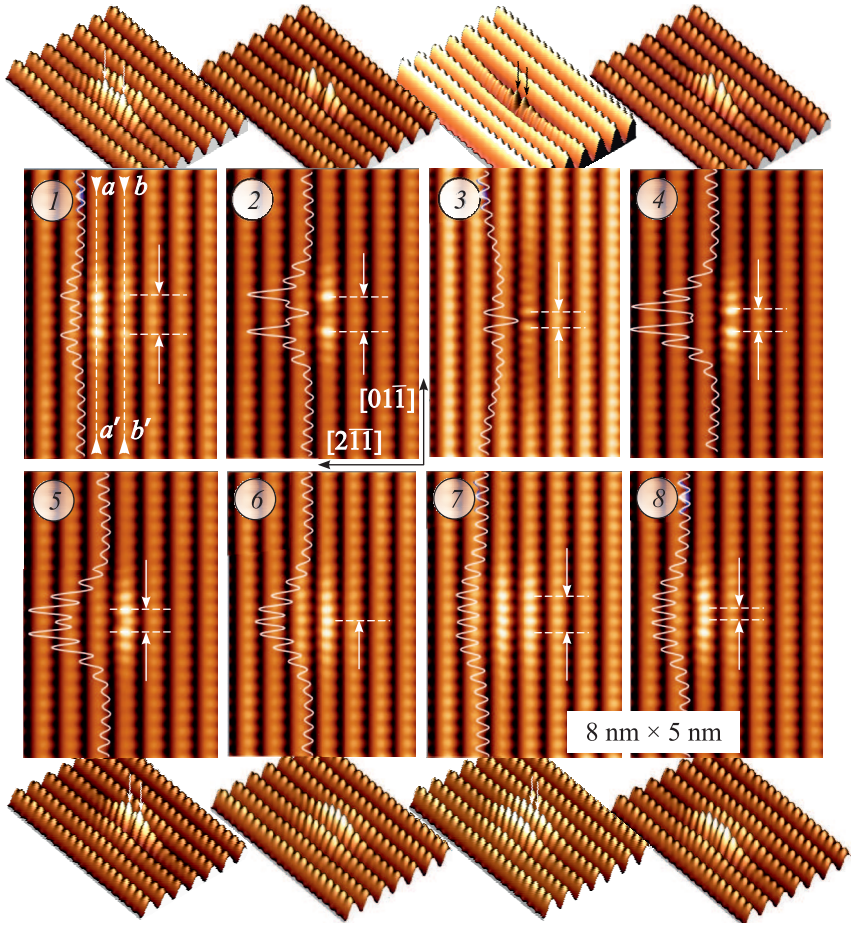

Fig. 6. $LDOS(x, y)$ maps in vicinity of P atom, located at different positions in subsurface layers of Ge(111)-(2×1) surface. Numbers denote atoms position

Thus, P donor impurity at position *1* is imaged as two row feature with two maxima in a row and double dimer distance between maxima.

Si(111)-(2×1) and Ge(111)-(2×1) surfaces are similar in many senses. At Si(111)-(2×1) surface π^* band is separated from valence band by 0.4 eV [7], and the surface is easier to analyze comparing to Ge(111)-(2×1) surface, where π^* band and VB overlap.

It is possible to perform a simple check of our results by comparison with Si(111)-(2×1) surface [7]. In accordance with Fig. 6 and Table the conclusions of authors can be immediately confirmed. In our notations: Fig. 2a [7] corresponds to P in position *2*, Fig. 2b [7] – P in position *4*, Fig. 2b [7] – P in position *5*. The remaining unclear feature (Fig. 2d [7]) most probably is the STM image of P atom, adsorbed on the surface. This statement is out of scope of present investigation and will be proved in the future publications [11].

The last problem we would like to discuss is the point spectroscopy $LDOS(eV)$ curves. The typical curve is depicted in Fig. 7 together with calculated $I(V)$ curve on a logarithmic scale.

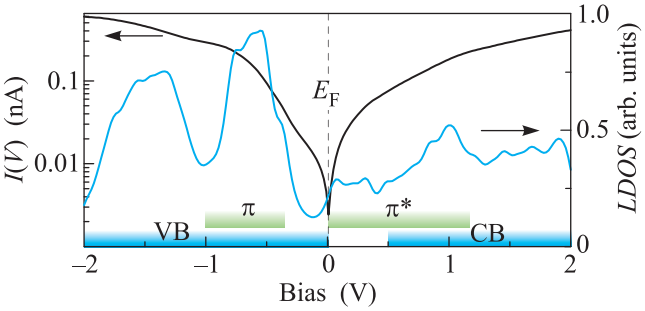

Fig. 7. The $LDOS(eV)$ curve and log(I(V)) (curve averaged above the whole 8×5 nm surface slab)

It is shown to demonstrate, that the surface band gap determination from spectroscopic data is not obvious task. There are no specific points of $I(V)$ curve (as well as on its derivative) which can be used for band gap definition.

Let us specify the strong assumptions used in present calculations. Some of them are imposed by very big simulation super-cell. In particular, we have performed the simulation in LDA approximation. It is known it gives non-physically small values of band gaps. This can be slightly improved by the GGA approximation, but real improvements can be achieved only with computationally expensive GW approximation [3]. There is no correction for closed STM feedback loop. The values of $LDOS$ are calculated on the *plane* above the surface. There is no STM tip density of states in our results. In our model we can not account for the surface band bending, we simply do not have sufficiently thick model slab. Our slab is about 15 Å thick, and the depletion layer at Ge(111)-(2×1) surface with n-type of bulk conductivity is almost 250 Å thick. The depletion layer strongly affects the picture of tunneling for heavily doped Ge samples [12]. The same concerns the Si.

That is why our model STM images do not coincide exactly with experimental observations, but nevertheless the correspondence is reasonable. All $LDOS(x, eV)$ maps (except position *3*) predicts the presence of protrusion on the STM images at zero (and small negative) bias voltage, which indeed agree with experiment [11]. We did not find any substantial difference when explicitly adding charge to the impurity atom.

In conclusion, we performed the numerical modeling of Ge(111)-(2×1) surface electronic properties in vicinity of P donor impurity atom near the surface. We show, that despite of well established bulk donor impurity energy level position at the very bottom of conduction band, surface donor impurity might produce energy level below Fermi energy, depending on impurity atom local environment. It was demonstrated, that impurity, located in subsurface atomic layers, is visible in STM experiment. The quasi-1D character of impurity image, observed in STM experiments, is confirmed by our computer simulations.

This work has been supported by RFBR grants and computing facilities of Moscow State University. We would also like to thank the authors of WxSM and Chimera free software.

1. E. Artacho, D. Sanchez-Portal, P. Ordejon et al., Phys. Stat. Sol. (b) **215**, 809 (1999).
2. S. V. Savinov, S. I. Oreshkin, and N. S. Maslova, JETP Lett. **93**(9), 521 (2011); S. V. Savinov, A. I. Oreshkin, and S. I. Oreshkin, JETP Lett. **96**(1), 31 (2012).
3. C. Violante, A. Mosca Conte, F. Bechstedt, and O. Pulci, Phys. Rev. B **86**, 245313 (2012).
4. K. Loser, M. Wenderoth, T. K. A. Spaeth et al., Phys. Rev. B **86**, 085303 (2012).
5. G. Bussetti, B. Bonanni, S. Cirilli et al., Phys. Rev. Lett. **106**, 067601 (2011).
6. J. K. Garleff, M. Wenderoth, K. Sauthoff, and R. G. Ulbrich, Phys. Rev. B **70**, 245424 (2004).
7. J. K. Garleff, M. Wenderoth, R. G. Ulbrich et al., Phys. Rev. B **76**, 125322 (2007).
8. J. M. Nicholls, P. Maartensson, and G. V. Hansson, Phys. Rev. Lett. **54**, 2363 (1985).
9. M. A. Olmstead and N. M. Amer, Phys. Rev. B **29**, 7048 (1984).
10. D. A. Muzychenko, S. V. Savinov, V. N. Mantsevich et al., Phys. Rev. B **81**, 035313 (2010).
11. S. V. Savinov et al., (to be published).
12. P. I. Arseyev, N. S. Maslova, V. I. Panov et al., JETP Lett. **82**(5), 279 (2005).